Journal of Alloys and Compounds 872 (2021) 159671

Contents lists available at ScienceDirect

Journal of Alloys and Compounds

journal homepage: www.elsevier.com/locate/jalcom

A zeolite-free synthesis of luminescent and photochromic hackmanites

Hannah Byron[a,b], Isabella Norrbo[a], Mika Lastusaari[a,c,*]

[a] University of Turku, Department of Chemistry, FI-20014 Turku, Finland
[b] University of Turku Graduate School (UTUGS), Doctoral Programme in Physical and Chemical Sciences, Turku, Finland
[c] Turku University Centre for Materials and Surfaces (MatSurf), Turku, Finland

ARTICLE INFO

Article history:
Received 11 January 2021
Received in revised form 2 March 2021
Accepted 22 March 2021
Available online 26 March 2021

Keywords:
Optical materials
Energy storage materials
Phosphors
Solid state reactions
Optical properties
Luminescence

ABSTRACT

In order to further boost their potential applications as optical materials by improving structural and compositional tuneability, hackmanites ($Na_8(AlSiO_4)_6(Cl,S)_2$) exhibiting multiple optical properties such as photoluminescence, persistent luminescence, and tenebrescence, were synthesised in a solid-state reaction using simple starting materials. All materials with the desired structure showed both blue-white photoluminescence typical of synthetic hackmanite, and white persistent luminescence, which have not previously been reported for hackmanites synthesised using zeolite-free methods. The typical orange luminescence of disulfide seen in natural hackmanites after 365 nm excitation was not observed. Samples made under optimised synthesis conditions of heating at 900 °C for 72 h followed by a reduction also showed purple tenebrescence typical of hackmanite. The optical energy storage properties of hackmanites made without zeolite A, as well as potential methods for tuning them, are discussed for the first time. These materials have previously been investigated for potential as multifunctional optical markers and for optical multiplexing; these results further the understanding of hackmanites and bring them one step closer to commercial viability as optical materials.

1. Introduction

First considered for the potential applications of its photo- and cathodochromic properties in the 1950s [1], synthetic hackmanite ($Na_8(AlSiO_4)_6(Cl,S)_2$) has in recent years seen its range of possible uses expand greatly. Many accounts of the synthesis of photo- and cathodochromic hackmanites have been given, with aims of producing materials suitable for applications ranging from cathodochromic cathode-ray tube (CRT) imaging plates, through optical data storage, to use as a pigment [2–4]. Other recent examples of photochromic materials to which hackmanite could be compared include molybdenum and tungsten oxides, as well as metal-organic frameworks [5–9].

While the striking reversible colour changes (i.e. tenebrescence) of natural hackmanites have inspired research for approximately the last 100 years, they boast at least three further optical properties. Natural hackmanites also show an orange fluorescence under UV light [10], and more recently, other properties of natural and synthetic hackmanites have been studied: namely a white photoluminescence (PL) and white persistent luminescence (PeL) [11–14]. This brings the total number of optical properties up to four, and along with an investigation into structural control of the tenebrescence [15], gives hackmanite great potential to serve as a robust and tuneable optical multiplexing material [16].

So far, a range of synthesis methods for hackmanite have been discussed, including hydrothermal and solid-state methods using varying starting materials [11,17–19]. Photochromic materials have been made using all of these methods, though only hackmanites made from zeolite A ($NaAlSiO_4$) have had their PL and PeL properties discussed thoroughly [11,12,20]. When used as a starting material, zeolite A contributes to the bulk of the hackmanite's composition, as shown in Eq. (1). This means that only the NaCl can easily be substituted, which limits the tunability of the material.

$$6\ NaAlSiO_4 + NaCl + Na_2SO_4 \rightarrow Na_8(AlSiO_4)_6(Cl,S)_2 \quad (1)$$

The research this work is based upon aimed to synthesise and characterise hackmanites exhibiting white PL, white PeL and tenebrescence using a zeolite-free method. It is not known whether any of the alternative, zeolite-free methods produced hackmanites with white PeL, as it has not previously been discussed. The synthesis method used in this work was based off that of Medved [18], the starting materials and exact heating temperatures and times being modified to produce hackmanites with all desired optical properties. This was done because by using simpler starting materials such as

* Corresponding author at: University of Turku, Department of Chemistry, FI-20014 Turku, Finland.
E-mail address: miklas@utu.fi (M. Lastusaari).

https://doi.org/10.1016/j.jallcom.2021.159671
0925-8388/

Al_2O_3, SiO_2 and Na_2O (in the form of NaOH or Na_2CO_3), the composition can be more finely tuned to produce materials with all the desired properties.

2. Materials and methods

2.1. Materials preparation

Samples were prepared using a solid-state reaction by mixing stoichiometric amounts of dried Al_2O_3 (Merck, Aluminium oxide 90 standardised), SiO_2 (Sigma, 99.8%), NaCl (Sigma Aldrich, 99.5%), Na_2SO_4 (E. Merck, 99%) and Na_2CO_3 (E. Merck, 99.5%) or NaOH (Merck, 99%) and grinding together by hand. H_3BO_3 (E. Merck, 99.8%) was added as a flux (10% by mass) to some samples. For solid-state synthesis, the mixtures were heated in air at 800–1060 °C for 48–72 h, then allowed to cool freely. Once cool, the mixtures were ground again and subsequently heated at 850 °C under a flowing 12% H_2/88% N_2 atmosphere for 2 h and allowed to cool. Samples were washed with distilled water to remove soluble impurities such as NaCl, and thoroughly dried.

2.2. Experimental methods

Structure and purity of the samples were assessed using room temperature X-ray powder diffraction measured with a Huber G670 detector and copper $K_{\alpha 1}$ radiation (λ = 1.54060 Å). Exposure time was 30 min, with 10 readings of the imaging plate. Sample compositions were investigated with X-ray fluorescence spectroscopy using a PANalytical Epsilon 1 device with internal Omnian calibration. Loss of chloride was investigated using thermogravimetric analysis, with a TA Instruments SDT Q600. Approximately 10 mg of reaction mixture was heated from 20° to 1300°C at a rate of 10 °C/min in air, flow rate 100 mL/min.

Crystallite sizes were estimated by analysing the most intense reflection (around 24.3°) using the Scherrer formula Eq. (2) [21,22]. In this formula, D = mean crystallite size, K = Scherrer constant, usually 0.89, λ = X-ray wavelength, β = full width at half maximum (FWHM) in radians and θ = half of 2θ. This formula assumes that broadening of the peak is due only to domain size, as well as that domains are spherical and there is no size distribution. This is largely true for very small domains (1–30 nm), however for larger crystallites the instrumental contribution to the signal width becomes significant, and thus it must be corrected for (Eq. (3) [22]). In this work, microcrystalline silicon was used for the corrections, with its FWHM being 0.140° for the setup used here. Note that this formula generally only holds for values of $D < 100$ nm, though the exact limit depends on the degree of instrumental broadening. The relationship between FWHM and domain size for the setup used in this work is shown in Fig. A.1.

$$D = K\lambda/\beta \cos\theta \quad (2)$$

$$\beta^2 = \beta\ sample^2 - \beta\ ref^2 \quad (3)$$

Photoluminescence and persistent luminescence spectra after UV excitation were measured at room temperature using a Varian Cary Eclipse Fluorescence Spectrophotometer containing a Hamamatsu R928 photomultiplier and a 150 W xenon lamp. The internal light source was used for the UV excited photoluminescence spectra, with a delay of 0.1 ms, excitation slit 10 nm, emission slit 2.5 nm and a gate time of 5 ms. For persistent luminescence spectra, samples were excited using 302 nm radiation from a UVP model UVM-57, 6 W lamp for 5 min at room temperature (irradiance approx. 2.3 mW cm^{-2}), followed by a 1 min delay before measurement. Persistent luminescence lifetimes were investigated using a Hagner ERP-105 luminance photometer at room temperature. Samples were excited with 302 nm radiation from the same lamp as previously mentioned, or 254 nm radiation from a UVP model UVLS-24 EL, 4 W 254/365 nm lamp for 30 min (irradiance approx. 2.3 mW cm^{-2} (302 nm), 3.1 mW cm^{-2} (254 nm)); measurement started immediately after irradiation ceased and continued until the luminance dropped below 0.3 mcd m^{-2}. Optical energy storage properties were investigated using thermoluminescence measurements with a MikroLab Thermoluminescent Materials Laboratory Reader RA'04. Samples were excited with 302 nm and 254 nm UV from the same lamps as previously mentioned for 5 min (dose approx. 1.7 mW cm^{-2} (302 nm), 1.3 mW cm^{-2} (254 nm)), and the thermoluminescence measurement taken using a heating rate of 9 °C s^{-1} after a 1 min delay. Preheated measurements were taken to investigate deep traps. Samples were excited for 5 min with a handheld 254 nm lamp, then preheated to between 180 and 250 °C. Preheated samples were measured using a heating rate of 9 °C s^{-1} 1 min after excitation ceased. Corrections to the glow curves to account for thermal quenching of luminescence were carried out (Fig. A.6a and b, Appendix A Section 5) [23]. All glow curves presented in this work are corrected, and corrected data were used to calculate trap depths.

The change of colour of the materials after UV irradiation was investigated using reflectance measurements under illumination of a 60 W incandescent lamp, with incident irradiance kept constant in all measurements. The reflectance of the sample before excitation was measured relative to Al_2O_3 as a white background colour. Samples were excited with 254 nm radiation from the same handheld lamp as previously discussed for 5 min (dose approx. 1.1 mW cm^{-2}) and their reflectance measured again 20 s after irradiation ceased to show the change in reflectance. The difference of the two reflectances was calculated to show the colour change. Spectra were collected using an Avantes FC-IR600–1-ME-HTX optical fibre connected to an Avantes AvaSpec-2084 × 14 spectrometer with a data collection time of 1.6 s. Cathodochromism was measured under the light of an Ocean Optics LS-1 Cal torch located approximately 3 cm from the sample. The reflectance of the sample before bombardment was measured relative to Al_2O_3 as the white background colour, and the sample was then subjected to an electron beam for 5 min using a Nuclide Corp. ELM2EX Luminoscope at 50–100 mTorr pressure. The reflectance was measured again 10 s after electron bombardment ceased using the same spectrometer as previously mentioned, with a data collection time of 1.6 s. The difference of the two reflectances was calculated to show the colour change.

3. Results and discussion

3.1. Purity and composition

The structure and purity of the materials was investigated using X-ray powder diffraction (pXRD). Results showed that most samples contained the expected sodalite structure; the only anomalous peak was caused by the sample mount, made of X-ray fluorescence (XRF) film and Vaseline (Fig. 1a). An exception to this was the sample made at 1060 °C, the synthesis temperature suggested in Medved's work on which this method was based [18]. At this temperature, chloride was lost from the structure and the resulting product was nepheline (ideal composition: $Na_3KAl_4Si_4O_{16}$) [24], an aluminosilicate material with very weak optical properties [25]. The potassium in this material is expected to have come from impurities in the starting materials. The loss of chloride is supported by XRF measurements, where significantly less chloride was detected for the sample made at 1060 °C compared to others with the correct structure (Table A.1). Thermogravimetric analysis (TGA) measurements also showed a decrease in mass beginning at 850 °C and ending at around 1000 °C thought to be due to the chloride escaping at these temperatures (Fig. 1b). Other features in the TGA curve have been identified as arising from the decomposition of Na_2CO_3 in the presence of SiO_2 [26].

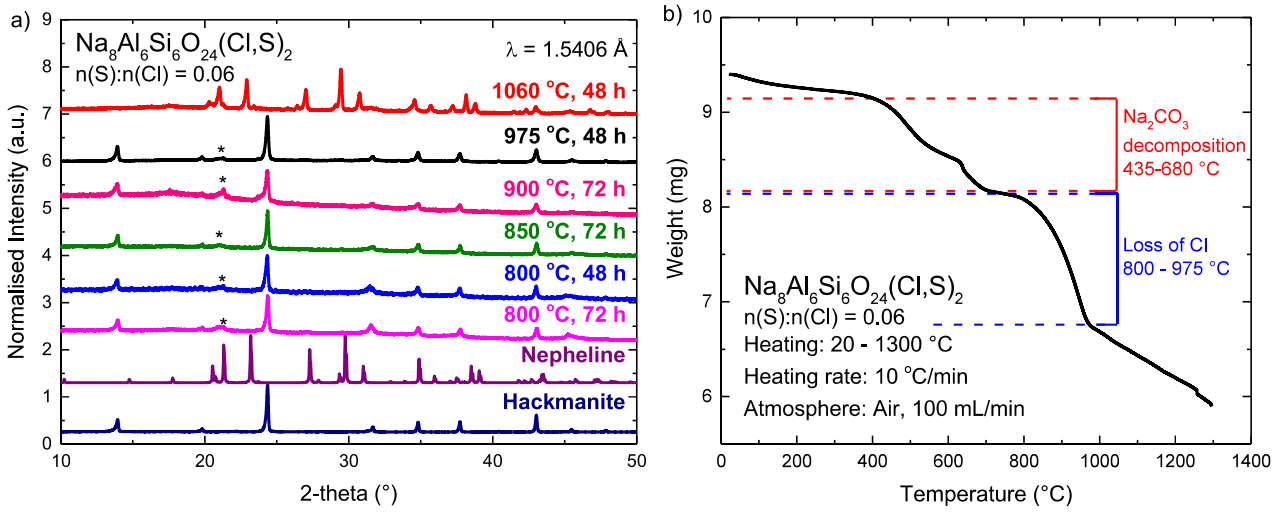

Fig. 1. (a) pXRD patterns for samples synthesised at 800–1060 °C for 48–72 h as shown, along with reference data for Nepheline (PDF 00-035-0424 (ICDD, 2018)) [24], and hackmanite made from zeolite A. * indicates a background peak from the sample mount. (b) TGA curve for the reaction mixture heated in air. The decomposition of Na_2CO_3 [26] and the region where loss of chloride occurs are indicated on the graph.

Crystallite sizes calculated using the Scherrer formula (Table 1) indicate that all the materials are nanocrystalline, i.e. the domain sizes are <100 nm in diameter. This is significant, because it is believed that nanocrystalline materials have weaker optical properties than if the domain size is >100 nm. The reasons for this are discussed later.

Both NaOH and Na_2CO_3 were used as a source of Na_2O in this work and compared directly to see which was the best starting material. Very little difference in structure, purity and quality of optical properties was noticed between the two (Table A.1, Fig. A.2a and b). Therefore, Na_2CO_3 was considered the better choice of starting material, since it is safer to handle and less hygroscopic than NaOH. Boric acid was also tested as a flux, since it had been used successfully in previous hackmanite syntheses based on zeolite A [12]. The addition of the flux was unsuccessful in this case, because it underwent a side reaction with the alumina and Na_2O source to produce $Na_2Al_2(B_2O_7)$ (Fig. A.2a).

3.2. Photo- and persistent luminescence

PL spectra of the samples made in this zeolite-free synthesis matched the expected profiles for hackmanite well. The characteristic blue-white photoluminescence was observed for all samples with the correct structure, with some spectra shown in Fig. 2. White photoluminescence of some synthetic sodalites caused by anionic oxygen species has been discussed by Doorn et al. [3], but more recently it has been shown that Ti^{3+} contributes more significantly to hackmanite's white PL [20]. In these materials, the presence of titanium arises from impurities in the alumina starting material. The white persistent luminescence of hackmanite shown to occur because of a Ti^{3+}/V_O pair is presented in Fig. 3 [20]. This white PeL has not previously been reported for hackmanites made using a zeolite-free synthesis, to the authors' best knowledge. The samples chosen for these figures also illustrate clearly the difference in luminescence intensity between optimised (900 °C, 72 h) and non-optimised (975 °C, 48 h) synthesis. The sample made at 1060 °C shows a very weak luminescence with emission maximum around 520 nm, excited by 254 nm (Fig. 2), but no blue-white luminescence and no afterglow. The lack of typical hackmanite luminescence fits with the absence of any sodalite structure visible for this sample (Fig. 1a), though some chloride was observed using XRF (Table A.1), suggesting a very small amount of hackmanite could still exist in this sample. The weak luminescence of this sample is thought to be from manganese: XRF data show a larger proportion of manganese in this sample (Table A.1), and manganese has been shown to have photoluminescence excitation and emission spectra close to those observed for this sample, when present in hackmanites and other aluminosilicate materials [3,20,27].

Table 1
Calculated crystallite sizes for samples synthesised at 800–975 °C for 48–72 h. and a reference made from zeolite A. Details of the calculation of the reference sample are found in Table A.2. [a]Actual domain size likely much larger than this (Appendix A Section 2).

Sample	*D*/nm
Reference	>>430[a]
975 °C, 48 h	63.2 ± 1
900 °C, 72 h	40.0 ± 1
850 °C, 72 h	79.8 ± 1
800 °C, 48 h	49.5 ± 1
800 °C, 72 h	62.0 ± 1

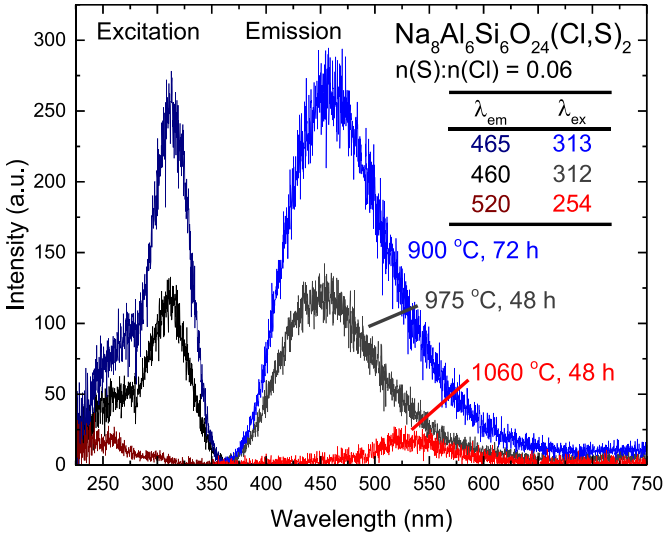

Fig. 2. Photoluminescence excitation and emission spectra for three samples made under conditions shown. The sample with the nepheline structure (red) shows different luminescence properties to hackmanite.

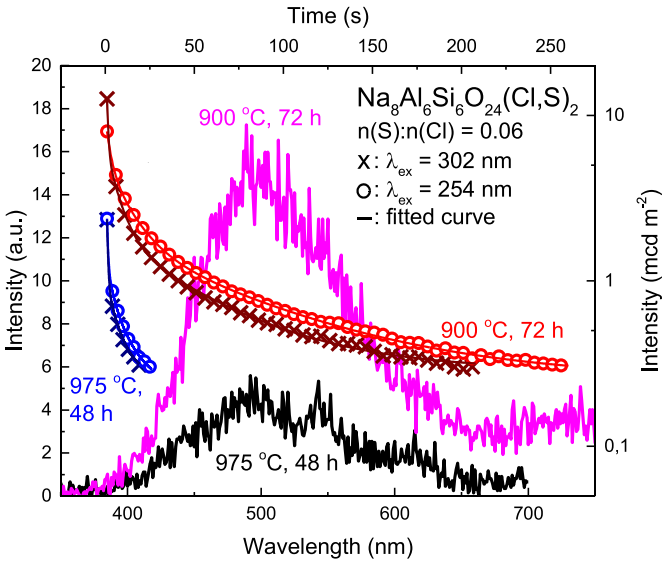

Fig. 3. Persistent luminescence spectra for the samples made under the conditions shown (bottom left axes, 302 nm t_{ex}: 5 min, t_{delay}: 1 min); luminance fading curves for the same samples after excitation with 302 nm and 254 nm UV light (top right axes, 30 min excitation).

PeL spectra showed peaks at the expected wavelength for afterglow given from a Ti^{3+}/V_O pair in hackmanite, i.e. 500 nm (Fig. 3) [20]. Lifetimes of PeL above a 0.3 mcd m^{-2} industrial threshold for safety lighting materials were measured for all samples [28], as this indicates how long the PeL is visible to the human eye in the dark. The best products lasted around 4 min above this threshold, and the poorest only a couple of seconds (Fig. 3, Table 2). Reference materials made from zeolite A have been known to have PeL lasting for many hours [12]. Unlike previous materials [11], these hackmanites showed the longest-lived PeL after irradiation with 254 nm light, rather than 302 nm. This is thought to be because of the lack of or weak tenebrescence in these materials. In samples with strong tenebrescence, most of the high energy UV is absorbed by polysulfide species and stored in the traps responsible for the purple tenebrescence, meaning little energy is left over to be stored in the Ti^{3+}/V_O pair, resulting in weaker afterglow. 302 nm radiation has enough energy to excite electrons to fill the PeL traps without filling the tenebrescence traps, meaning PeL is usually stronger after irradiation with 302 nm light. However, when the tenebrescence is weak, the higher energy 254 nm light can easily excite electrons to populate the PeL traps and give rise to strong PeL.

The PeL process is thought to have several components, as the decay curves are best fitted with exponential curves having 2 or 3 terms. The general formula for the decay process as a function of intensity vs time is given in Eq. (4). In this formula, I = intensity, A_n = amplitude, t = time and τ_n = time constant. The time constants for each decay curve are given in Table 2, as well as the length of time the luminescence is at an intensity of greater than 0.3 mcd m^{-2} (indicated as Lifetime in the table).

Table 2
Persistent luminescence fading time constants and length of time luminescence is measured to be above 0.3 mcd m^{-2}.

λ_{ex}/nm	τ_1/s	τ_2/s	τ_3/s	Lifetime/s
975 °C, 48 h				
254	0.58 ± 0.03	3.7 ± 1.3	13 ± 6	25
302	0.57 ± 0.01	6.7 ± 0.3	–	19
900 °C, 72 h				
254	2.51 ± 0.08	12.5 ± 0.04	75 ± 2	259
302	0.75 ± 0.01	7.1 ± 0.2	51 ± 1	198

Table 3
Trap depth data calculated from the glow curves in Fig. 4 using the initial rise method. Shallow traps were calculated from the 302 nm glow curves, deep traps from the 254 nm preheated glow curves. Trap depth values have been corrected for thermal quenching [23].

Trap type	Trap E_A /× 10^{-20} J	Trap depth/eV	Glow curve maximum/°C
975 °C, 48 h			
Shallow	7.9 ± 0.2	0.50 ± 0.01	184
Deep	17 ± 2	1.0 ± 0.1	301
900 °C, 72 h			
Shallow	8.5 ± 0.1	0.53 ± 0.01	207
Deep	–	–	–
850 °C, 72 h			
Shallow	5.9 ± 0.5	0.37 ± 0.03	179
Deep	9 ± 2	0.6 ± 0.1	267
800 °C, 48 h			
Shallow	5.5 ± 0.8	0.34 ± 0.05	170
Deep	11.2 ± 0.6	0.72 ± 0.04	280
800 °C, 72 h			
Shallow	5.7 ± 0.5	0.36 ± 0.03	175
Deep	9.1 ± 0.8	0.57 ± 0.05	269

$$I(t) = A_1 \exp(-t/\tau_1) + A_2 \exp(-t/\tau_2) + A_3 \exp(-t/\tau_3) \quad (4)$$

The persistent luminescence and PL of these samples was generally weaker than that of materials made using zeolite A, including the reference sample made during this work. One reason for this is that all the samples made with the zeolite-free route were nanocrystalline (Table 3) while the one made from zeolite A was not. This is significant because when the crystallite is small enough, the contribution of the surface on luminescence quenching becomes important. For small crystallites, a significant number of energy transfer pathways can lead to the surface, where the energy is lost non-radiatively [29]. Contrary to this expectation, within this group of nanocrystalline samples the longest lived PeL was recorded in the material made at 900 °C for 72 h (40.0 nm), whereas those with larger calculated domain sizes had much shorter lived PeL (Fig. 3). This suggests that while crystallite size has a strong effect, there are also other factors that influence both PL and PeL in hackmanites. Since hackmanites' PL and PeL rely on the presence of Ti^{3+}/V_O pairs, it seems that the sample with the smallest crystallites has the best defect structure, allowing the formation of such pairs.

The optical energy storage of these materials and PeL processes were further investigated using thermoluminescence measurements. Several of the materials showed more than one trap when irradiated by 254 nm UV, with this deeper trap only being populated when higher energy UV was used (Fig. 4). After the glow curves were corrected for thermal quenching of luminescence, the initial rise method was used to analyse the glow curves and obtain activation energies and trap depths for these materials [30]. The portion of the curves analysed in this way was the initial region where luminescence was between 5% and 15% of the maximum intensity. Deep traps' glow curves were isolated using preheating to allow for analysis using the initial rise method. The calculated trap depths are shown in Table 3; most of these are close to values measured for hackmanites made from zeolite in other publications [12,20]. For shallow traps, the observed trend was that higher synthesis temperatures as well as longer heating times deepen these traps. In the case of the deeper traps, the greatest trap depths were observed for samples heated for a shorter time, i.e. only 48 h. In the case of the material made at 900 °C for 72 h (the optimised synthesis), no deep trap was present at all. This is evident from the preheated curve being wholly beneath both the 302 nm and 254 nm glow curves, suggesting its peak is only due to residual energy stored in the shallow trap not fully released on preheating, rather than energy in a separate deeper trap. This sample also shows more intense

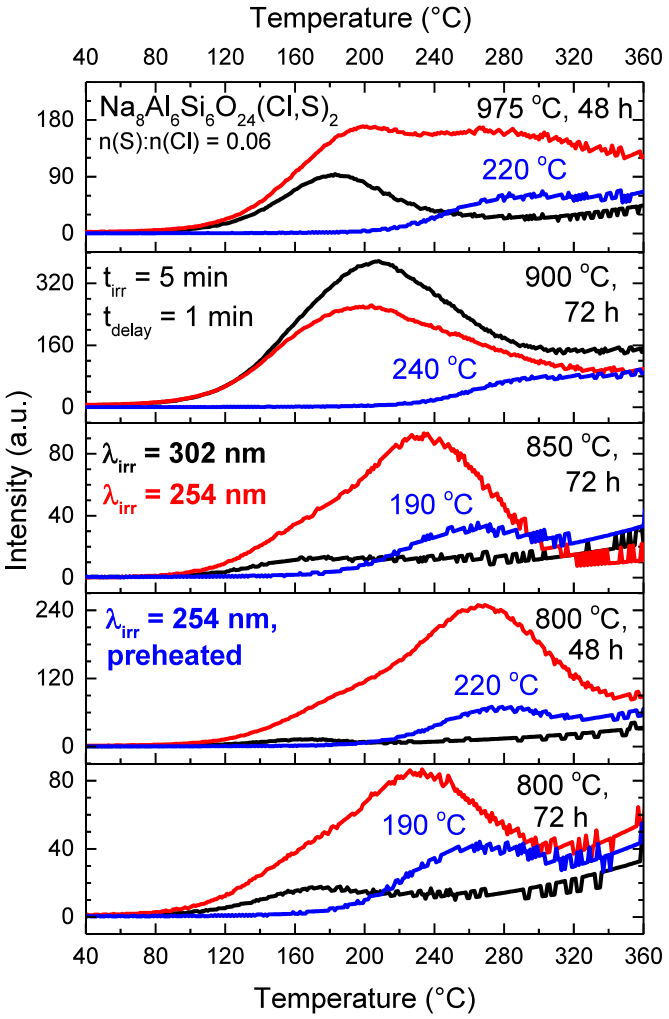

Fig. 4. Glow curves measured after irradiation with 302 nm, 254 nm, and 254 nm with preheating. Preheating temperatures are indicated in blue above their respective curves. Glow curves have been corrected for thermal quenching (Appendix A Section 5) [23].

thermoluminescence after irradiation with 302 nm light, possibly because it is tenebrescent, meaning some of the 254 nm photons were stored in tenebrescence traps rather than PeL traps.

The trends in trap depth data here suggest that the synthesis conditions could be changed in order to tune the material for various applications. For example, those with a greater density of shallow traps could be used as long persistent phosphors, whereas those with more of the deeper traps could function as materials used in dosimetry.

3.3. Tenebrescence

Tenebrescence is a mineralogical term for reversible photochromism. The tenebrescence in hackmanite has been shown to arise from excitation of an electron from sulfide impurities in the structure into a chloride vacancy on exposure to UV radiation [13,20,31,32]. An F centre is formed, and the purple colour appears because of absorption of green light by the F centre. The colour can then be fully bleached either thermally or optically, returning the material to its original non-coloured form. A mechanism for this is shown in Fig. 5a [13].

Only samples made at 900 °C showed any visible tenebrescence. This is possibly because at this temperature, enough chloride leaves the structure to make space for the low oxidation state sulfur species, but not so much that the structure changes from sodalite to nepheline. Samples made below this temperature did not show any tenebrescence, and neither did those made above this temperature even if they still had the correct structure. Another possibility is that this temperature and heating time is a sweet spot for the correct hackmanite structure, including the required defects for tenebrescence, to form from the simple starting materials. The tenebrescence colouration was investigated by measuring the sample's reflectance before and after colouration to see how this changed. The difference was also calculated to illustrate more clearly the change in reflectance (Fig. 5b). All tenebrescent samples showed a shift and deepening of the reflectance minimum from 500 nm to 530–560 nm, corresponding to change from light brown to purple. These materials were able to change colour after irradiation with 254 nm UV light. The non-white body colours of the materials made in this work are thought to be the result of a combination of sulfur species forming yellow, blue and pink chromophores in the non-coloured state, independent from the F centre responsible for tenebrescence (Appendix A Section 6, Fig. A.7a and b) [33].

These materials also exhibit cathodochromism, i.e. they change colour when subjected to a beam of electrons. Cathodochromic sodalites have been reported several times since the 1970s made using a range of methods such as solid-state and hydrothermal [3,4,17,34,35],

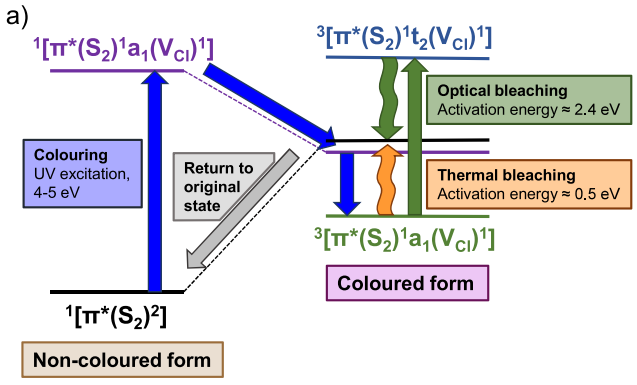

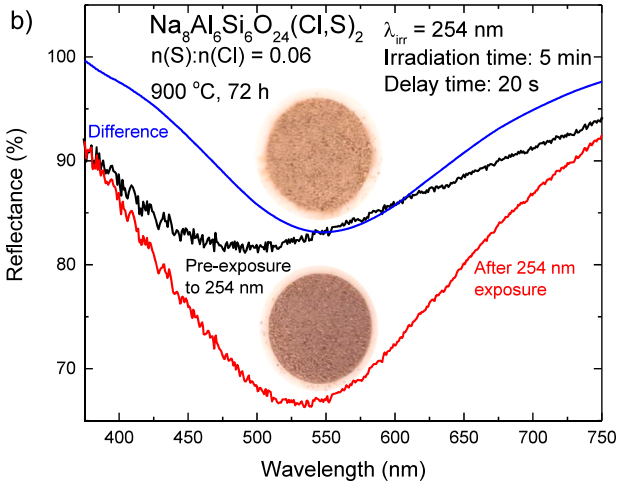

Fig. 5. (a) Mechanism for the tenebrescence in hackmanite, showing both colouration and bleaching of the colour [13]. (b) Reflectance curves of a sample made at 900 °C for 72 h before and after UV irradiation, and the difference between them. Photographs of the sample before (top) and after (bottom) irradiation are displayed to show the colour change.

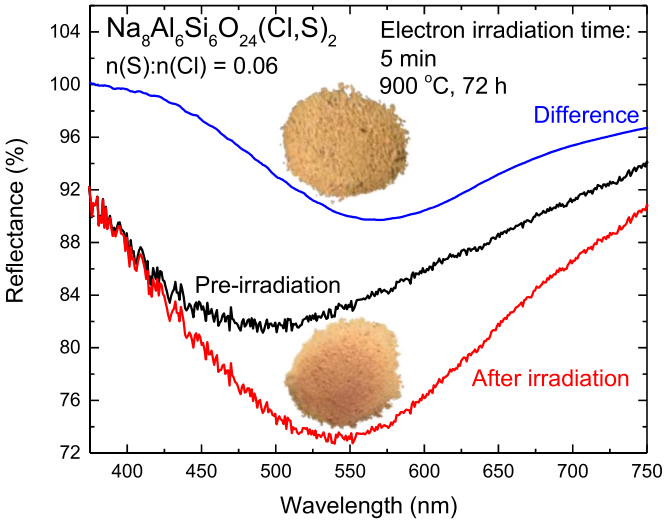

Fig. 6. Reflectance curves of a sample made at 900 °C for 72 h before and after being subjected to an electron beam, and the difference between them. Photographs of the sample before (top) and after (bottom) irradiation are displayed to show the colour change.

and were suggested as potentially useful for developing cathodochromic cathode ray tube displays [2]. In this work, little to no colouration was observed for most materials after 5 min of electron bombardment, detectable only by a spectrometer (Fig. A.5), though for the materials displaying visible tenebrescence, clear cathodochromism was also observed (Fig. 6).

4. Conclusions

In this work, the synthesis parameters for producing luminescent and tenebrescent hackmanites using a zeolite-free solid-state method are defined to be: heating at 900 °C for 72 h in air, followed by a 2 h reduction at 850 °C under 12% H_2:88% N_2. To the authors' best knowledge, this is the first account of the persistent luminescent and optical energy storage properties of hackmanites made in this way; these and the photoluminescence properties were found to match well those of hackmanites made using zeolite A as discussed in the literature. The impact of different synthesis conditions using this method on the product's optical properties are discussed, such as the effect of heating temperature and time on the number and depth of shallow and deep thermoluminescence traps in the materials. It was found that conducting the synthesis at too high a temperature, i.e. >1000 °C, resulted in loss of chloride, changing the structure and properties of the final product completely. This observation was supported by the results of TGA, where the loss of chloride is clearly visible. These results are inconsistent with the results of Medved [18], whose paper this method was based on. In his work, synthesis at 1060 °C is claimed to produce a tenebrescent sodalite – in this work, only samples made at the optimal 900 °C showed any tenebrescence.

The simpler starting materials make compositional changes much easier, leading to more possibilities of tuning the material chemically. For example, up to all 8 sodium atoms could be replaced with Li, K, Rb or other cations, where previously only nominally 2 of these could be substituted due to the composition of zeolite A [12,13]. Cl, S, Al and Si could also be replaced relatively easily for other elements. This could lead to simultaneous tuning of for example tenebrescence colour and luminescence properties, which have only been discussed separately thus far [12,15]. Future work would involve trying to synthesise samples differing in composition to basic hackmanite ($Na_8(AlSiO_4)_6(Cl,S)_2$, n(S):n(Cl) = 0.06) to investigate the effect on tenebrescence and persistent luminescence, in line with previous observations [12,13]. These materials could also be doped with Ti to improve luminescence properties [20].

Efforts to develop hackmanite into a commercially viable, low-cost and highly tuneable material with multiple optical properties continue. This work brings to light some more ways in which hackmanite can be tuned, both through altering synthesis conditions and by improving compositional tunability. This in turn brings hackmanite one step closer to becoming an everyday material, serving purposes such as in optical multiplexing, UV indexing, safety lighting and diagnostics.

Funding

This work was supported by Business Finland (project 6479/31/2019).

CRediT authorship contribution statement

Hannah Byron: Conceptualization, Methodology, Investigation, Writing - original draft. **Isabella Norrbo**: Conceptualization, Supervision, Writing - review & editing. **Mika Lastusaari**: Conceptualization, Supervision, Writing - review & editing.

Declaration of Competing Interest

The authors declare that they have no known competing financial interests or personal relationships that could have appeared to influence the work reported in this paper.

Acknowledgements

Thanks also go to Sami Vuori for assistance in the setup and use of specialised laboratory equipment.

Appendix A. Supporting information

Supplementary data associated with this article can be found in the online version at doi:10.1016/j.jallcom.2021.159671.

References

[1] T.E. Warner, Synthesis, Properties and Mineralogy of Important Inorganic Materials, Wiley, Somerset, GB, 2011.
[2] L.T. Todd, A. Linz, E.F. Farrell, Cathodochromic CRT employing faceplate-deposited sodalite and electron-beam erase, IEEE Trans. Electron Devices 22 (1975) 788–792, https://doi.org/10.1109/T-ED.1975.18220
[3] C.Z. van Doorn, D.J. Schipper, P.T. Bolwijn, Optical investigation of cathodochromic sodalite, J. Electrochem. Soc. 119 (1972) 85–92, https://doi.org/10.1149/1.2404141
[4] W. Phillips, Properties of cathodochromic sodalite, J. Electrochem. Soc. 117 (1970) 1557–1561, https://doi.org/10.1149/1.2407383
[5] N.K. Kulachenkov, D. Sun, Y.A. Mezenov, A.N. Yankin, S. Rzhevskiy, V. Dyachuk, A. Nominé, G. Medjahdi, E.A. Pidko, V.A. Milichko, Photochromic Free MOF-Based Near-Infrared Optical Switch 59 Angewandte Chemie International Edition, 2020, pp. 15522–15526, https://doi.org/10.1002/anie.202004293
[6] N. Li, Y. Li, G. Sun, Y. Zhou, S. Ji, H. Yao, X. Cao, S. Bao, P. Jin, Enhanced photochromic modulation efficiency: a novel plasmonic molybdenum oxide hybrid, Nanoscale 9 (2017) 8298–8304, https://doi.org/10.1039/C7NR02763J
[7] Z. Shao, Q. Wu, X. Han, Y. Zhao, Q. Xie, H. Wang, H. Hou, Proton coupled electron transfer: novel photochromic performance in a host–guest collaborative MOF, Chem. Commun. 55 (2019) 10948–10951, https://doi.org/10.1039/C9CC05498G
[8] P.-X. Li, Z.-X. Xie, A.-P. Jin, J. Li, G.-C. Guo, A new photochromic Gd-MOF with photoswitchable bluish-white to greenish-yellow emission based on electron transfer, Chem. Commun. 56 (2020) 14689–14692, https://doi.org/10.1039/D0CC06019D
[9] Y. Shen, L. Pan, Z. Ren, Y. Yang, Y. Xiao, Z. Li, Nanostructured WO_3 films synthesized on mica substrate with novel photochromic properties, Journal of Alloys and Compounds 657 (2016) 450–456, https://doi.org/10.1016/j.jallcom.2015.10.103
[10] D. Kondo, D. Beaton, Hackmanite/Sodalite from Myanmar and Afghanistan, Gems Gemol. 45 (2009) 38–43, https://doi.org/10.5741/GEMS.45.1.38
[11] I. Norrbo, P. Gluchowski, P. Paturi, J. Sinkkonen, M. Lastusaari, Persistent luminescence of tenebrescent $Na_8Al_6Si_6O_{24}(Cl,S)_2$: multifunctional optical markers,

Inorg. Chem. 54 (2015) 7717–7724, https://doi.org/10.1021/acs.inorgchem.5b00568
[12] I. Norrbo, J.M. Carvalho, P. Laukkanen, J. Mäkelä, F. Mamedov, M. Peurla, H. Helminen, S. Pihlasalo, H. Härmä, J. Sinkkonen, M. Lastusaari, Lanthanide and heavy metal free long white persistent luminescence from Ti doped Li-hackmanite: a versatile, low-cost material, Adv. Funct. Mater. 27 (2017) 1606547, https://doi.org/10.1002/adfm.201606547
[13] I. Norrbo, A. Curutchet, A. Kuusisto, J. Mäkelä, P. Laukkanen, P. Paturi, T. Laihinen, J. Sinkkonen, E. Wetterskog, F. Mamedov, T. Le Bahers, M. Lastusaari, Solar UV index and UV dose determination with photochromic hackmanites: from the assessment of the fundamental properties to the device, Mater. Horiz. 5 (2018) 569–576, https://doi.org/10.1039/C8MH00308D
[14] C. Agamah, S. Vuori, P. Colinet, I. Norrbo, J.M. de Carvalho, L.K. Okada Nakamura, J. Lindblom, L. van Goethem, A. Emmermann, T. Saarinen, T. Laihinen, E. Laakkonen, J. Lindén, J. Konu, H. Vrielinck, D. Van der Heggen, P.F. Smet, T.L. Bahers, M. Lastusaari, Hackmanite—the natural glow-in-the-dark material, Chem. Mater. 32 (2020) 8895–8905, https://doi.org/10.1021/acs.chemmater.0c02554 https://doi.org/10.1021/acs.chemmater.0c02554.
[15] E.R. Williams, A. Simmonds, J.A. Armstrong, M.T. Weller, Compositional and structural control of tenebrescence, J. Mater. Chem. 20 (2010) 10883–10887, https://doi.org/10.1039/c0jm02066d
[16] I. Norrbo, I. Hyppänen, M. Lastusaari, Up-conversion luminescence – a new property in tenebrescent and persistent luminescent hackmanites, J. Lumin. 191 (2017) 28–34, https://doi.org/10.1016/j.jlumin.2017.02.046
[17] L. T. Todd Jr., E. F. Farrell, A. Linz, Process for Preparing Cathodochromic Sodalite, 3,932,592, 1976.
[18] D.B. Medved, Hackmanite and its tenebrescent properties, Am. Miner. 39 (1954) 615–629.
[19] E.F. Williams, W.G. Hodgson, J.S. Brinen, Synthetic photochromic sodalite, J. Am. Ceram. Soc. 52 (1969) 139–144, https://doi.org/10.1111/j.1151-2916.1969.tb11200.x
[20] I. Norrbo, P. Gluchowski, I. Hyppänen, T. Laihinen, P. Laukkanen, J. Mäkelä, F. Mamedov, H.S. Santos, J. Sinkkonen, M. Tuomisto, A. Viinikanoja, M. Lastusaari, Mechanisms of tenebrescence and persistent luminescence in synthetic hackmanite $Na_8Al_6Si_6O_{24}(Cl,S)_2$, ACS Appl. Mater. Interfaces 8 (2016) 11592–11602, https://doi.org/10.1021/acsami.6b01959
[21] J.I. Langford, A.J.C. Wilson, Scherrer after sixty years: a survey and some new results in the determination of crystallite size, J. Appl. Cryst. 11 (1978) 102–113.
[22] L. Alexander, H.P. Klug, Determination of crystallite size with the X-ray spectrometer, J. Appl. Phys. 21 (1950) 137–142, https://doi.org/10.1063/1.1699612
[23] K. Van den Eeckhout, A.J.J. Bos, D. Poelman, P.F. Smet, Revealing trap depth distributions in persistent phosphors, Phys. Rev. B 87 (2013) 045126, https://doi.org/10.1103/PhysRevB.87.045126
[24] Int. Cent. Diffr. Data, PDF-4 + 2018, entry 00-035-0424 (Nepheline).
[25] A.A. Finch, Conversion of nepheline to sodalite during subsolidus processes in alkaline rocks, Mineral. Mag. 55 (1991) 459–463, https://doi.org/10.1180/minmag.1991.055.380.15
[26] B. Dong, Y. Xu, S. Lin, X. Dai, Characterizing and exploring the formation mechanism of salt deposition by reusing advanced-softened, silica-rich, oilfield-produced water (ASOW) in superheated steam pipeline, Sci. Rep. 5 (2015) 17274, https://doi.org/10.1038/srep17274
[27] Luminescent Minerals, in: M. Gaft, R. Reisfeld, G. Panczer (Eds.), Modern Luminescence Spectroscopy of Minerals and Materials, Springer, Berlin, Heidelberg, 2005, pp. 45–118, https://doi.org/10.1007/3-540-26377-2_4
[28] Phosphorescent pigments and products – Part 1: Measurement and marking at the producer. DIN 67510–1:2009–11, Berlin, Germany, (2009).
[29] F. Wang, J. Wang, X. Liu, Direct Evidence of a Surface Quenching Effect on Size-Dependent Luminescence of Upconversion Nanoparticles, 49 Angewandte Chemie International Edition, 2010, pp. 7456–7460, https://doi.org/10.1002/anie.201003959
[30] A. Bos, Thermoluminescence as a research tool to investigate luminescence mechanisms, Materials 10 (2017) 1357, https://doi.org/10.3390/ma10121357
[31] R.D. Kirk, Role of sulfur in the luminescence and coloration of some aluminosilicates, J. Electrochem. Soc. 101 (1954) 461–465, https://doi.org/10.1149/1.2781301
[32] D.J. Schipper, C.Z.V. Doorn, P.T. Bolwijn, Preparation of cathodochromic sodalites, J. Am. Ceram. Soc. 55 (1972) 256–259, https://doi.org/10.1111/j.1151-2916.1972.tb11275.x
[33] A.A. Finch, H. Friis, M. Maghrabi, Defects in sodalite-group minerals determined from X-ray-induced luminescence, Phys. Chem. Miner. 43 (2016) 481–491, https://doi.org/10.1007/s00269-016-0816-7
[34] C.E. Stroud, J.M. Stencel, L.T. Todd, Infrared spectra of cathodochromic sodalite, J. Phys. Chem. 83 (1979) 2378–2382, https://doi.org/10.1021/j100481a015
[35] T. Takeda, A. Watanabe, Optically erasable cathodochromic coloration in sodalites containing sulfate, J. Electrochem. Soc. 120 (1973) 1414–1418, https://doi.org/10.1149/1.2403272